SU(3)-guided realistic nucleon-nucleon interactions for large-scale calculations

G. H. Sargsyan,[1] K. D. Launey,[1] R. B. Baker,[1] T. Dytrych,[1,2] and J. P. Draayer[1]
[1]*Department of Physics and Astronomy, Louisiana State University, Baton Rouge, Louisiana 70803, USA*
[2]*Nuclear Physics Institute, 250 68 Rez, Czech Republic*

(Received 25 September 2020; revised 11 February 2021; accepted 3 March 2021; published 2 April 2021)

We examine nucleon-nucleon realistic interactions, based on their SU(3) decomposition to SU(3)-symmetric components. We find that many of these interaction components are negligible, which, in turn, allows us to identify a subset of physically relevant components that are sufficient to describe the structure of low-lying states in ^{12}C and related observables, such as excitation energies, electric quadrupole transitions, and rms radii. We find that paring down the interaction by half or more yields results that practically coincide with the corresponding *ab initio* calculations with the full interaction. In addition, we show that while various realistic interactions differ in their SU(3) decomposition, their renormalized effective counterparts exhibit a striking similarity and composition that can be linked to dominant nuclear features such as deformation, pairing, clustering, and spin-orbit effect.

DOI: 10.1103/PhysRevC.103.044305

I. INTRODUCTION

Ab initio calculations aim to describe nuclear features while employing high-precision interactions that describe two- and three-nucleon systems (often referred to as "realistic interactions"), such as those derived from meson exchange theory [1,2] (e.g., CD-Bonn [3]), chiral effective field theory [4–6] (e.g., NNLO$_{\rm opt}$ [7] and N3LO [8]), or J-matrix inverse scattering (JISP16 [9,10]). As such calculations do not depend on any information about the nucleus in consideration, these methods can be used in nuclear regions where experimental data are currently sparse or not available, e.g., along the pathways of nucleosynthesis and toward a further exploration of exotic physics of rare isotopes.

While realistic interactions build upon rich physics at the nucleon-nucleon (NN) level, it is impossible to identify terms in the interaction that are responsible for emergent dominant features in nuclei, such as deformation, pairing, and clustering. These features, which are revealed in even the earliest of data on nuclear structure, have informed many successful nuclear models such as Elliott's SU(3) model [11–13] and the Bohr collective model [14] with a focus on deformation, as well as algebraic [15,16] and exact [17] pairing models. Recently, we have shown that calculations that consider Hamiltonians that build upon the ones used in these earlier studies and, in addition, allow for configuration mixing [18–20], yield results that are consistent with the ones in the *ab initio* symmetry-adapted no-core shell model (SA-NCSM) [21,22]. In particular, the no-core symplectic model (NCSpM) has offered successful descriptions for excitation energies, monopole and quadrupole transitions, quadrupole moments, and rms radii for a range of nuclei (from $A = 8$ to $A = 24$ systems, including cluster effects in the ^{12}C Hoyle state) [18,19,23], by employing quadrupole-quadrupole ($Q \cdot Q$) and spin-orbit interaction terms. In Ref. [20], exact solutions to the shell model plus isoscalar and isovector pairing have been provided for low-lying 0^+ states and, e.g., the energy of the lowest isobaric analog state in ^{12}C has been shown to agree with the corresponding *ab initio* findings. Therefore, it is interesting to trace this similarity in outcomes to specific features of the realistic interactions.

In this paper, we provide new insight into correlations within realistic interactions through the use of the deformation-related SU(3) symmetry. Specifically, we show that only a part of the nucleon-nucleon interaction appears to be essential for the description of nuclear dynamics, especially at low energies. When expressed in the SU(3) symmetry-adapted basis, the interaction—given as SU(3) tensors—shows a clear preference toward a specific subset of tensors, allowing us to determine its dominant components. Most importantly, these features appear regardless of the underlying theory used to construct the interaction. Furthermore, an almost universal behavior is revealed by "soft-core" potentials such as JISP16, or by the renormalized ("softened") counterparts of "harder" interactions that use, e.g., Okubo-Lee-Suzuki (OLS) [24,25] and similarity renormalization group (SRG) [26] renormalization techniques. And further, to complete the picture, we show that these features are directly linked to the important physics, i.e., deformation, clustering, pairing, and spin-orbit effects, that drove the development of earlier, and considerably simpler, schematic models.

The importance of various interaction components is studied in SA-NCSM calculations. In particular, we study nuclear structure observables of ^{12}C, such as the low-lying excitation spectrum, $B(E2)$ reduced transition probabilities and root mean square (rms) radii. We compare the results that use the entire interaction with those that use interactions that have been selected down to their dominant components. The agreement observed for all these observables is remarkable, even when a small fraction of the interaction is used.

II. THEORETICAL METHOD

A. SA-NCSM framework

It was shown in the recent study by Dytrych *et al.* [22] that only a few dominant configurations in symmetry-adapted (SA) basis are sufficient to describe most of the physics in nuclei. Similar patterns were also seen in, e.g., Refs. [27]. These configurations correspond to equilibrium shapes with their vibrations and rotations that can be described within the SA collective basis. This lays the foundation of the *ab initio* SA-NCSM, which is a no-core shell model with an SU(3)-coupled or Sp(3, $\mathbb{R}$)-coupled symmetry-adapted basis (for a recent review, see Refs. [21,22] and the references therein). Similarly to NCSM [28,29], it uses a harmonic oscillator (HO) basis, where the HO major shells are separated by a parameter $\hbar\Omega$. The model space is capped by an $N_{\max}$ cutoff which is the maximum total number of oscillator quanta above the lowest HO configuration for a given nucleus. The SA-NCSM utilizes a non relativistic nuclear Hamiltonian with translationally invariant interactions plus Coulomb interaction. Since we work in laboratory coordinates, we remove the spurious center-of-mass excitation states from the low-lying spectrum with a Lawson term [30,31]. The model calculates eigenvalues and eigenvectors of the nuclear interaction Hamiltonian and subsequently uses the eigenvectors for calculations of the nuclear observables. The results approach the exact value as the $N_{\max}$ increases, and at the $N_{\max} \to \infty$ limit they become independent of the HO parameter $\hbar\Omega$. Within a given complete $N_{\max}$ model space, the SA-NCSM results exactly match those of the NCSM for the same interaction. The use of symmetries in the SA-NCSM allows one to select the model space by considering only the physically relevant subspace, which is only a fraction of the corresponding complete $N_{\max}$ space.

In the SA-NCSM, the SA basis is constructed using an efficient group-theoretical algorithm for each HO major shell [32]. While we do not use explicit construction of conventional NCSM bases, for completeness we show the unitary transformation from a two-particle JT-coupled basis state to an SU(3)-coupled state:

$$
\begin{aligned}
&|\eta_r\eta_s\omega\kappa(LS)\Gamma M_\Gamma\rangle \\
&= \frac{1}{\sqrt{1+\delta_{\eta_r\eta_s}}}\left\{a^\dagger_{(\eta_r\,0)\frac{1}{2}} \times a^\dagger_{(\eta_s\,0)\frac{1}{2}}\right\}^{\omega\kappa(LS)\Gamma M_\Gamma}|0\rangle \\
&= \frac{1}{\sqrt{1+\delta_{\eta_r\eta_s}}}\sum_{\substack{l_r l_s\\ j_r j_s}} \Pi_{j_r j_s LS}\langle(\eta_r\,0)l_r;(\eta_s\,0)l_s\|\omega\kappa L\rangle \\
&\quad\times\begin{Bmatrix} l_r & l_s & L\\ 1/2 & 1/2 & S\\ j_r & j_s & J\end{Bmatrix}\{a^\dagger_r \times a^\dagger_s\}^{\Gamma M_\Gamma}|0\rangle\,, \qquad (1)
\end{aligned}
$$

where we use conventional labels $r(s) = \{\eta(l\,\frac{1}{2})jt = \frac{1}{2}\}$; $\Gamma = JT$, with $\eta = 0, 1, 2, \ldots,$ is the HO shell number; $\Pi_j = \sqrt{2j+1}$; and $a^\dagger_{(\eta\,0)\frac{1}{2}} \equiv a^\dagger_{\eta\frac{1}{2}}$ is the creation operator that creates a particle of spin $\frac{1}{2}$ in a HO major shell η corresponding to an $(\eta\,0)$ state in the SU(3) basis. We use SU(3) quantum numbers, $\omega \equiv (\lambda\,\mu) = (\eta_r\,0) \times (\eta_s\,0)$, $\tilde{\omega} \equiv (\mu\,\lambda)$, and κ distinguishes multiple occurrences of the same total orbital momentum L for a given ω. The two states are coupled through reduced SU(3) Clebsch-Gordan coefficients $\langle;\|\rangle$ [33,34]. S is the total intrinsic spin of the two-particle system and we use the Wigner 9-j symbol.

To provide a more detailed description of the SU(3) quantum numbers ω, as discussed in Ref. [21], the single-particle HO basis states $|\eta l m_l\rangle$, can be expressed by $|\eta_z\eta_x\eta_y\rangle$, with $\eta_z + \eta_x + \eta_y = \eta$. For a given HO shell η, the complete shell-model space is then specified by all distinguishable distributions of η_z, η_x, and η_y. For example, for $\eta = 2$ there are 6 distinct distributions, $(\eta_z, \eta_x, \eta_y) = (2, 0, 0)$, $(1, 1, 0)$, $(1, 0, 1)$, $(0, 2, 0)$, $(0, 1, 1)$, and $(0, 0, 2)$. Each of these configurations can be occupied by maximum of two spin-$\frac{1}{2}$ particles of the same type. Adding (η_z, η_x, η_y) for all particles yields $(\eta_z^{\rm tot}, \eta_x^{\rm tot}, \eta_y^{\rm tot})$, with SU(3) quantum numbers given by $\lambda = \eta_z^{\rm tot} - \eta_x^{\rm tot}$ and $\mu = \eta_x^{\rm tot} - \eta_y^{\rm tot}$. For example, in the case of two particles in $\eta = 2$, if both are in $(2, 0, 0)$ configuration, then $\eta_z^{\rm tot} = 4$, $\eta_x^{\rm tot} = 0$ and $\eta_y^{\rm tot} = 0$, hence $(\lambda\,\mu) = (4\,0)$,: if one of the particles is in $(2, 0, 0)$ and the other is in $(1, 1, 0)$, then $\eta_z^{\rm tot} = 3$, $\eta_x^{\rm tot} = 1$, and $\eta_y^{\rm tot} = 0$, resulting in $(\lambda\,\mu) = (2\,1)$. Thus, by indicating the difference between the HO quanta in each direction, these labels relay important information about nuclear deformation.

B. SU(3) interaction tensors

NN interactions can be divided into components that respect certain symmetries, such as rotational invariance. Two-body isoscalar (charge-independent) interactions are typically given in a representation of a JT-coupled HO basis, $|rs\Gamma M_\Gamma\rangle$, that is, $V^\Gamma_{rstu} = \langle rs\Gamma M_\Gamma = 0|V|tu\Gamma M_\Gamma = 0\rangle$. This takes advantage of the fact that the interaction transforms as a scalar under rotations in coordinate and isospin space, that is, it is an SO(3)$\times$ SU(2)$_T$ tensor of rank zero ($J_0 = 0, T_0 = 0$).

Analogously, the interaction can be represented in an SU(3) $\times$ SU(2)$_S$ $\times$ SU(2)$_T$-coupled HO basis $|\eta_r\eta_s\omega\kappa(LS)\Gamma M_\Gamma\rangle$ shown in Eq. (1). The corresponding interaction matrix elements are similarly given as $V^\Gamma_{(\chi\omega\kappa LS)_{fi}} \equiv \langle(\chi\omega\kappa(LS)\Gamma M)_f|V|(\chi\omega\kappa(LS)\Gamma M)_i\rangle$, with $\chi \equiv \{\eta_r\eta_s\}$ and with symmetry properties $V^\Gamma_{(\chi\omega\kappa LS)_{if}} = V^\Gamma_{(\chi\omega\kappa LS)_{fi}}$. The initial and final values of $(\chi\omega\kappa LS)_{if}$ can be different, i.e., the SU(3)$\times$SU(2)$_S$ rank of V is nonzero. In addition, since $J_0 = 0$, we have $L_0 = S_0$, thus the label L_0 will be henceforth omitted. Using the fact that the interaction can be represented as a sum of SU(3)$\times$SU(2)$_S$ tensors, $V = \sum_{\rho_0\omega_0\kappa_0 S_0} V^{\rho_0\omega_0\kappa_0 S_0}$, the matrix elements can be further reduced with respect to SU(3) and the spin-isospin space (for $T_0 = 0$), $V^{\rho_0\omega_0\kappa_0 S_0}_{(\chi\omega S)_{if};T} \equiv \langle(\chi\omega S)_f;T||V^{\omega_0\kappa_0 S_0}||(\chi\omega S)_i;T\rangle_{\rho_0}$ (see the Appendix). Here, the superscripts show the rank of the SU(3)$\times$SU(2)$_S$ tensor, and ρ_0 is the multiplicity that distinguishes between multiple occurrences of ω_0 for the same ω_i and ω_f.

The following conjugation relations hold for the SU(3) $\times$ SU(2)$_S$ tensors:

$$
\begin{aligned}
V^{\rho_0\omega_0\kappa_0 S_0}_{(\chi\omega S)_{if};T} &= (-)^{S_i - S_f + S_0}(-)^{\omega_f - \omega_i}\sqrt{\frac{\dim\omega_f}{\dim\omega_i}}V^{\rho_0\tilde{\omega}_0\kappa_0 S_0}_{(\chi\omega S)_{fi};T}\,,\\
V^{\rho_0\omega_0\kappa_0 S_0}_{(\chi\omega S)_{ii};T} &= (-)^{S_0}V^{\rho_0\tilde{\omega}_0\kappa_0 S_0}_{(\chi\omega S)_{ii};T}\,, \qquad (2)
\end{aligned}
$$

where

$$\dim\omega = \tfrac{1}{2}(\lambda+1)(\mu+1)(\lambda+\mu+2). \tag{3}$$

To simplify the equations in the paper, we introduce a symmetrized tensor,

$$v^{\rho_0\omega_0\kappa_0 S_0}_{(\chi\omega S)_{if};T} = (-)^{\omega_i - S_i - T}\sqrt{\dim\omega_i}\,V^{\rho_0\omega_0\kappa_0 S_0}_{(\chi\omega S)_{if};T}, \tag{4}$$

with a conjugation relation,

$$v^{\rho_0\omega_0\kappa_0 S_0}_{(\chi\omega S)_{if};T} = (-)^{S_0} v^{\rho_0\tilde{\omega}_0\kappa_0 S_0}_{(\chi\omega S)_{fi};T}. \tag{5}$$

We note that, in the case when $\chi_i = \chi_f$, $\omega_i = \omega_f$, and $S_i = S_f$, we will use the notation $v^{\rho_0\omega_0\kappa_0 S_0}_{(\chi\omega S);T}$.

C. Strength of SU(3) interaction tensors

The significance of the various SU(3) tensors can be estimated by their Hilbert-Schmidt norm, which is analogous to the norm of a matrix A defined as $||A|| = \sqrt{\sum_{ij} A_{ij}A_{ji}}$. In particular, the strength of a Hamiltonian H can be estimated by the norm σ_H constructed as [36–41]

$$\sigma_H^2 = \langle (H - \langle H\rangle)^\dagger (H - \langle H\rangle)\rangle = \langle H^2\rangle - \langle H\rangle^2, \tag{6}$$

where $\langle\cdots\rangle \equiv \frac{1}{\mathcal{N}}\mathrm{Tr}(\cdots)$ specifies the trace of the Hamiltonian matrix divided by the number $\mathcal{N}$ of diagonal matrix elements. In the present study, H is a two-body Hamiltonian, and $\mathcal{N}$ enumerates all possible two-particle configurations.

For given $T_f = T_i = T$ and a $|\chi^*\omega\kappa(LS)\Gamma M_\Gamma\rangle$ basis with $\chi^* \equiv \{\eta_r\eta_s\}$, $\eta_r \leqslant \eta_s$, the norm $\sigma_{\omega_0\kappa_0 S_0;T}$ of each SU(3)-symmetric tensor is determined using Eq. (6):

$$\sigma^2_{\omega_0\kappa_0 S_0;T} = \frac{1}{\mathcal{N}}\sum_{(\chi^*\omega S)_{f,i}\rho_0}\frac{1}{\Pi^2_{TS_0}\dim\omega_0}\left|v^{\rho_0\omega_0\kappa_0 S_0}_{(\chi\omega S)_{if};T}\right|^2 - \left(V_c^{\omega_0\kappa_0 S_0;T}\right)^2, \tag{7}$$

where the number of two-particle basis states, $\mathcal{N}$, and the average monopole part $V_c^{\omega_0\kappa_0 S_0} = \langle V^{\omega_0\kappa_0(L_0=S_0S_0)\Gamma_0=0M_{\Gamma_0}=0}\rangle$ are given, respectively, as

$$\mathcal{N} = \sum_{\chi^*\omega\kappa LSJM_J} 1 = \sum_{\chi^*\omega S}\Pi_S^2\dim\omega, \tag{8}$$

$$V_c^{\omega_0\kappa_0 S_0} = \frac{1}{\mathcal{N}}\sum_{\substack{\chi^*\omega\kappa\\ LSJ\rho_0}}\frac{\Pi_J^2\Pi_L}{\Pi_{S_0T}\sqrt{\dim\omega}}(-1)^{S_0+L+J-T-\omega} \times\begin{Bmatrix} L & S & J\\ S & L & S_0\end{Bmatrix}\langle\omega\kappa L;\omega_0\kappa_0 L_0\|\omega\kappa L\rangle_{\rho_0} v^{\rho_0\omega_0\kappa_0 S_0}_{(\chi\omega S);T}. \tag{9}$$

For a given isospin T, the strength of the entire Hamiltonian H_T is determined by the strengths of its components, $\sigma^2_{H_T} = \sum_{\omega_0\kappa_0 S_0}\sigma^2_{\omega_0\kappa_0 S_0;T}$. We can then define a relative strength for each SU(3)-symmetric component $(\omega_0\kappa_0 S_0)$ as

$$\mathfrak{s}^2_{\omega_0\kappa_0 S_0;T} = \frac{\sigma^2_{\omega_0\kappa_0 S_0;T}}{\sigma^2_{H_T}} = \frac{\sigma^2_{\omega_0\kappa_0 S_0;T}}{\sum_{\omega_0\kappa_0 S_0}\sigma^2_{\omega_0\kappa_0 S_0;T}}. \tag{10}$$

Using Eq. (A3), we can decompose any two-body interaction into SU(3)-symmetric components. The contribution of each of the components within the interaction is given by its relative strength (10) (see Fig. 1 for the realistic JISP16 and N3LO interactions). As can be seen from these results, only a small number of SU(3) tensors dominate the interaction, with the vast majority of the components having less than 1% of the total strength. The most dominant term, i.e., $(\lambda_0\,\mu_0) = (0\,0)$ is the one that preserves the SU(3) symmetry, which provides a further support of the successful Elliott model [11,12]. Various dominant terms will be discussed in detail in Sec. III B. Similar behavior is observed for other interactions. It should be noted that, in the JT-coupled basis, no such dominance of interaction matrix elements is apparent. This exercise demonstrates a long-standing principle that holds across all of physics; namely, one should work within a framework that is as closely aligned with the dynamics as possible [43].

III. RESULTS AND DISCUSSIONS

A. Observables in ^{12}C

The decomposition of the interaction in the SU(3) basis allows us to choose sets of major components to construct new selected interactions. These interactions can be used for calculations of various nuclear properties that can then be compared to the results from the initial interaction. In this way, we can examine how sensitive specific nuclear properties are to the interaction components.

Several selected interactions were constructed for this study. The selection is done by ordering the interaction tensors from the highest relative strength to the lowest and then including the largest ones to add up to 60–90% of the initial total strength. Depending on the $N_{\max}$ of the interaction the number of selected SU(3) tensors differs. For example, the JISP16 interaction in $N_{\max} = 10$, $\hbar\Omega = 15$ MeV has overall 169 unique $(\lambda_0\mu_0)S_0$ tensors, out of which the 51 largest ones account for about 80% of the total strength. After selection the total strengths are not rescaled to the initial interaction. Throughout this work we will refer to selected interactions in terms of the fraction of interaction tensors kept; that is, the number of SU(3)-symmetric components in the selected interaction relative to the number of all such components in the initial interaction for a given $N_{\max}$ and $\hbar\Omega$.

Analysis of the results shows that low-lying excitation energies of ^{12}C are not sensitive to the number of selected SU(3) tensors, given that the most dominant ones are included in the interaction (Fig. 2). With only half of the interaction tensors the excitation energies essentially do not differ from the corresponding results that use the full interaction, and even with less than 30% of the interaction components the deviation for most of the values is insignificant. The comparatively large deviation in 4^+ energy for $N_{\max} = 6$ that happens when about 20% of the SU(3) components are used is likely due to the small model space. This issue disappears in higher $N_{\max}$ values, and even $N_{\max} = 6$ results for the 2^+ state compare remarkably well to the initial interaction for all selections.

The selected interactions yield very close results to the initial one for other observables as well. For example, the ^{12}C rms radius of the ground state and the $B(E2: 2^+ \to 0^+)$ have very low dependence on the selection (Fig. 3), with variations

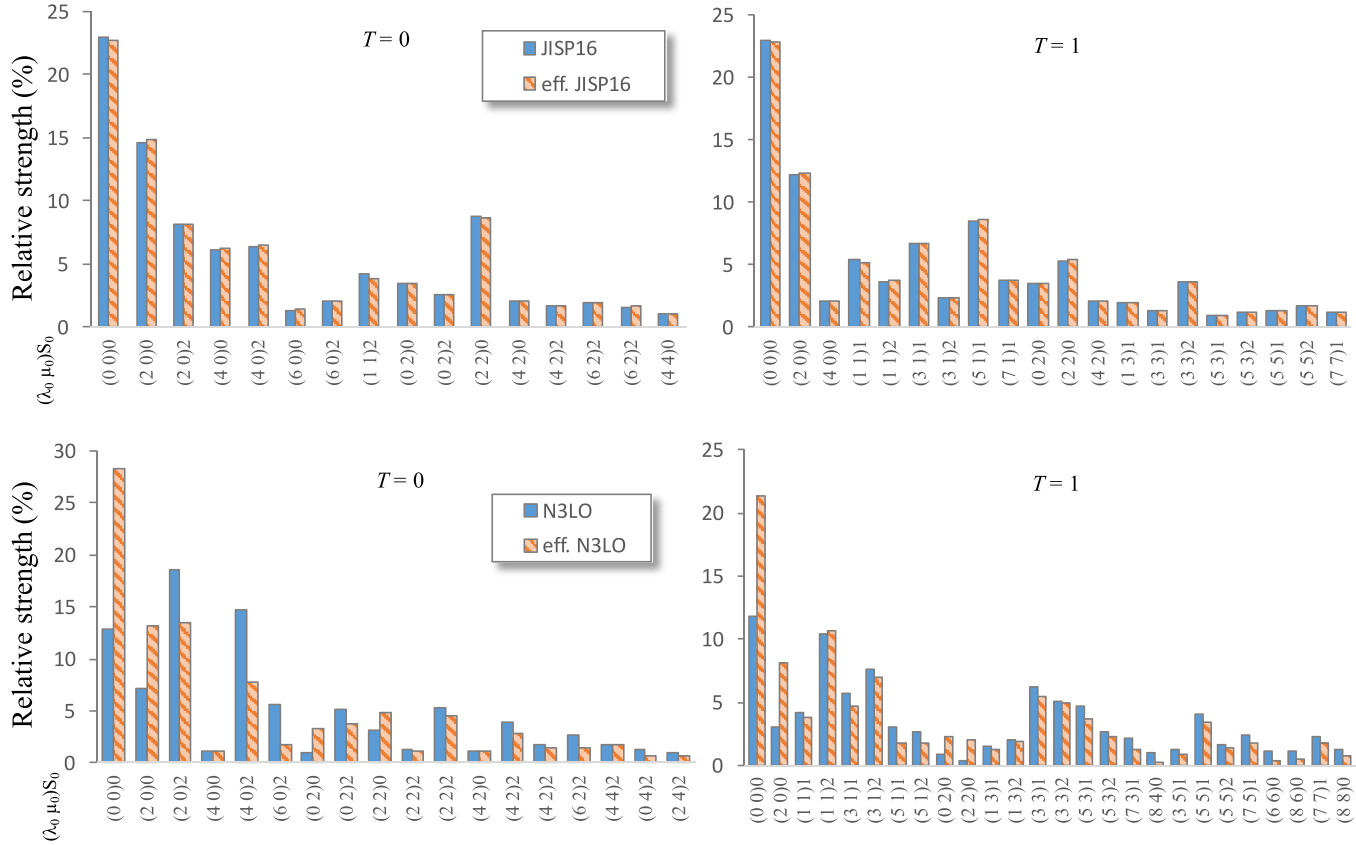

FIG. 1. Relative strengths $\mathfrak{s}$ (in %) for the SU(3)-coupled JISP16 (top) and N3LO (bottom) NN interactions and their effective counterparts with $\hbar\Omega = 15$ and 20 MeV, respectively, in the $N_{\max} = 6$ model space. The "eff. JISP16" is obtained by the OLS technique for $A = 12$, while "eff. N3LO" is by SRG with $\lambda_{\rm SRG} = 2.0$ fm^{-1}. T is the isospin of the two-nucleon system. A set of $(\lambda_0\mu_0)S_0$ quantum numbers and its conjugate correspond to each of the interaction terms. Only terms with >1% relative strength for each T are shown; there are more than 120 terms with less than 1% strength for this model space.

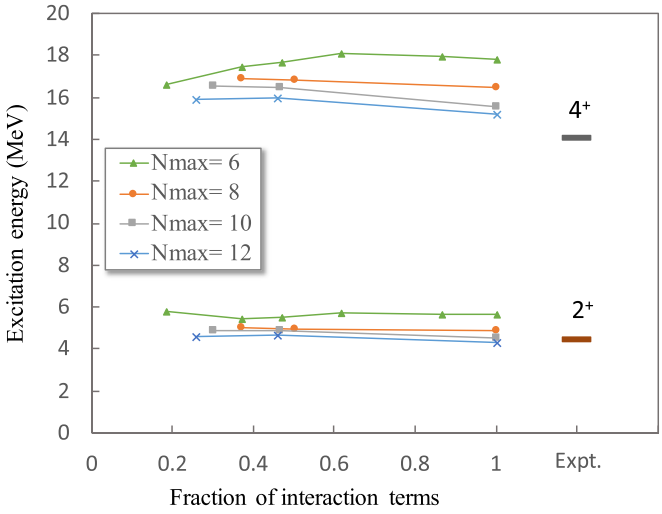

FIG. 2. Excitation energy of the first 2^+ and 4^+ states in ^{12}C from SA-NCSM calculations (connected lines) as a function of the fraction of the terms kept in the interaction, and compared to experiment [35] (labeled as "Expt."). Results for $N_{\max} = 6$, 8, 10, and 12 are shown for various selections of the JISP16 interaction with $\hbar\Omega = 15$ MeV. Specifically, the value 1 on the abscissa indicates that the full interaction (100%) was used, while an abscissa value of 0.4 implies that only the most significant 40% of the tensors were retained, etc.

nearly inconsequential compared to the deviations from the experiment (the underprediction of these observables for the JISP16 interaction has been addressed, e.g., in Ref. [31]). Specifically, the values are essentially the same when half of the interaction components are used. With less than 30% of interaction components, the difference from the initial interaction results is less than 2% for rms radius and less than 7% for $B(E2)$. Thus, small deviations start to appear only at significantly trimmed interactions, indicating that the long-range physics is mostly preserved when only the dominant interaction terms are used.

In addition, vital information about the nuclear structure can be found through analysis of the $(\lambda\mu)S$ configurations that comprise the SA-NCSM wave function. This uncovers the physically relevant features that arise from the complex nuclear dynamics as shown in Ref. [21]. In other words, the wave functions contain a manageable number of major SU(3) components that account for most of the underlying physics. Indeed, we find that calculations with various selected interactions largely preserve the major components of the wave function (Fig. 4). For the ground state of ^{12}C calculated in the $N_{\max} = 12$ model space the probability amplitude for each set of the quantum numbers $(\lambda\mu)S$ almost does not change when a little less then half (46%) of the JISP16 interaction tensors are used for the calculations. Even with about quarter

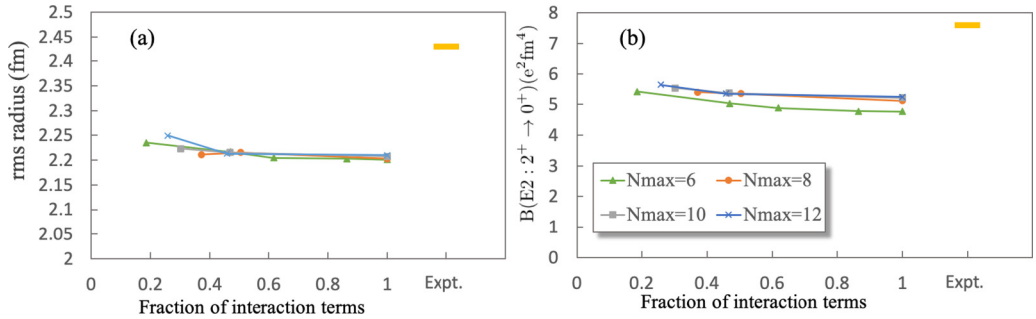

FIG. 3. Same as Fig. 2, but for the rms radius (in fm) of the ^{12}C ground state (experimental value from Ref. [42]) and the $B(E2 : 2_1^+ \to 0_1^+)$ value (in $e^2\text{fm}^4$) (experimental value from [35]) as a function of the fraction of the terms kept in the interaction. SA-NCSM calculations use various selections for the JISP16 interaction for $\hbar\Omega = 15$ MeV and different $N_{\max}$ model spaces.

(26%) of the tensors, the SU(3) structure remains the same with only a slight difference in the amplitudes. It should be noted that the $(\lambda\mu)S$ here are not to be confused with the ones in Fig. 1, as they correspond to the many-body states of ^{12}C. In particular, (0 4)0 is the lowest particle configuration in the HO basis, that is, four particles in $(\eta_z, \eta_x, \eta_y) = (1, 0, 0)$ and four particles in (0, 1, 0). As shown in Fig. 4, this accounts for almost half of the probability amplitude of the ground state wave function. The first three $(\lambda\mu)S$ in the figure correspond to the zero-particle–zero-hole (0p-0h) configurations, among which the (0 4)0 is the most deformed and has the lowest spin. The dominance of configurations with largest deformation and lowest spin has been shown in Ref. [21].

As mentioned above, the dependence on the HO parameter $\hbar\Omega$ disappears at the $N_{\max} \to \infty$ limit; however, even for comparatively small $N_{\max}$ model spaces, there is often a range of $\hbar\Omega$ values which achieves convergence for selected observables, while typically larger $N_{\max}$ model spaces are required outside this range. For long-range observables, such a range often falls close to an empirical estimate given by $\hbar\Omega = 41/A^{1/3}$ [14], which is 18 MeV for ^{12}C. We investigate the dependence of the ground state rms radius of ^{12}C on $\hbar\Omega$ using different selections (Fig. 5). We examine small model spaces, where the $\hbar\Omega$ dependence is large and its effect on the interaction selections is expected to be enhanced; yet, we ensure that these model spaces provide results close to the $N_{\max} = 12$ outcomes (see $N_{\max} = 6$ and 8 results in Figs. 2 and 3). Comparing to the full interaction, the results indicate that, indeed, small deviations are observed for values around $\hbar\Omega = 18$ MeV, and the deviations become larger at higher (less optimal) $\hbar\Omega$ values (Fig. 5). Similarly, the excitation energies for $\hbar\Omega = 15$ MeV calculations are much less sensitive to the interaction selection (Fig. 6),whereas the deviation in the results between the initial and selected interactions increases for higher $\hbar\Omega$. However, this difference gets smaller with increasing model space. To summarize, the selection of the interactions affects the calculations with optimal $\hbar\Omega$ values the least.

It is interesting to examine how the selection of NN interactions affects the nucleon-nucleon physics. As a simple illustration, we study the Hamiltonian for the proton-neutron system and its corresponding eigenvalues. (We note that states beyond the lowest 1^+ state are scattering states, but they

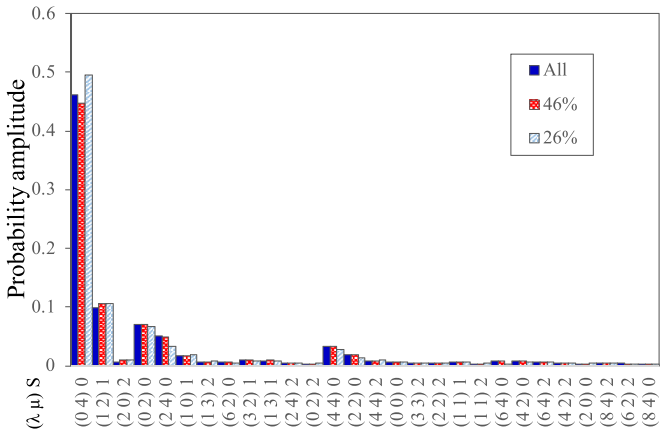

FIG. 4. Probability amplitudes for the $(\lambda\,\mu)S$ configurations that make up the ^{12}C ground state (0_1^+), calculated in $N_{\max} = 12$ model space using JISP16 interaction for $\hbar\Omega = 15$ MeV (labeled by "All") and two selected interactions (labeled by the fraction of the interaction components kept, 46% and 26%). Only states with probability amplitudes >0.003 are shown.

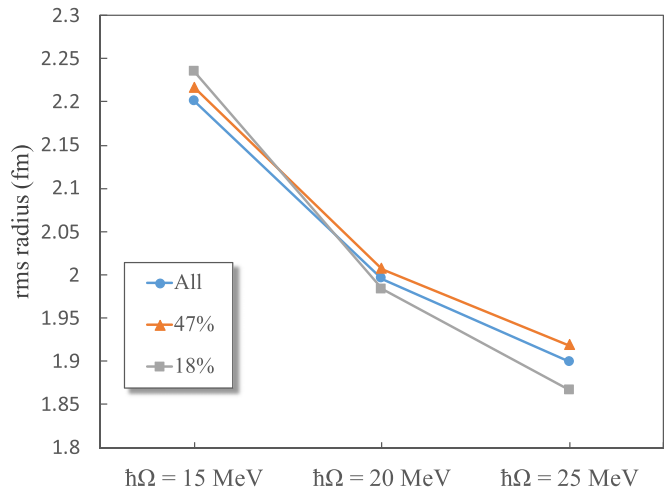

FIG. 5. ^{12}C ground state rms radius from SA-NCSM calculations with $N_{\max} = 6$ model space vs $\hbar\Omega$, using the full ("All") and selected (labeled by the percentage of the tensors kept) JISP16 interaction.

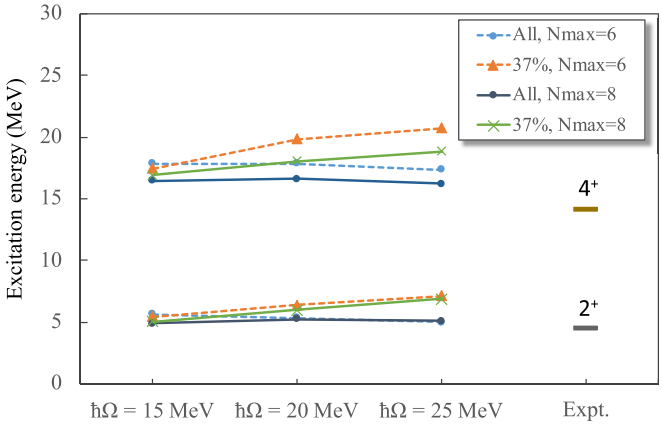

FIG. 6. Excitation energies of the first 2^+ and 4^+ states for ^{12}C from SA-NCSM calculations with $N_{\max} = 6$ and $N_{\max} = 8$ model spaces using full JISP16 interaction ("All") and its selected counterpart (with 37% of the tensors kept), with $\hbar\Omega = 15$, 20, and 25 MeV, and compared to experiment.

appear in a shell model energy spectra as distinct states; however, the idea here is to examine if there is any loss of information in the selected NN interaction, which in turn guides *ab initio* calculations.) In addition to $T = 0$ states, we consider $T = 1$ states, which can also inform the proton-proton and neutron-neutron systems. To do this, we look for deviations in the corresponding eigenvalues as compared to those computed with the full interaction.

In particular, we observe that only about quarter of the SU(3)-symmetric interaction components (the most dominant ones) can reproduce, with high accuracy, the energies that use the full interaction for most of the low-lying states of the proton-neutron system (Fig. 7). To estimate the difference in energies, we calculate the root mean square error (RMSE), $\text{RMSE} = \sqrt{\frac{1}{N_d}\sum_i^{N_d}(E^i_{\text{all}} - E^i_{\text{sel}})^2}$, where E_{all} and E_{sel} are the eigenenergies calculated with the initial and selected interactions, respectively, the summation is over all positive- or

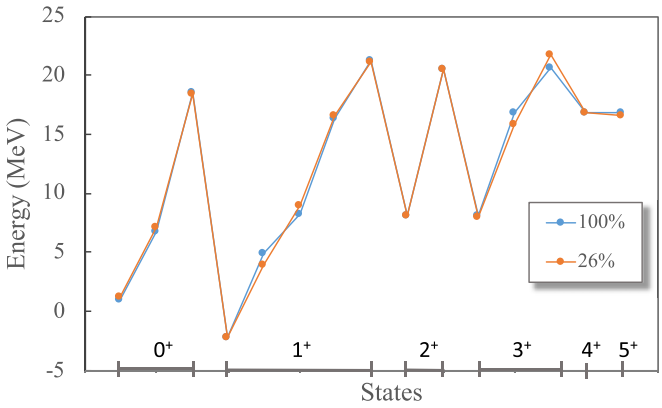

FIG. 7. Energies of the proton-neutron system for the positive-parity lowest-lying states (<30 MeV), calculated in the SA-NCSM in $N_{\max} = 12$ model space using the JISP16 interaction, with all terms kept (100%) as compared to a selection that keeps only 26% of the terms, for $\hbar\Omega = 15$ MeV.

negative-parity states, and N_d is the total number of states. For negative-parity $0 \leqslant J \leqslant 5$ states with energy up through 30 MeV, we find RMSE to be about 0.9–1.2 MeV depending on $\hbar\Omega$, whereas for positive-parity states it is between 0.5 and 0.9 MeV. Similar RMSE values are seen even for the higher lying spectrum up to 50 MeV. As it can be seen from Fig. 7, the main deviations come from the second and third 1^+ and 3^+ states, indicating that certain states are more sensitive to the selection than others.

B. Dominant features in realistic interactions

There are various techniques of renormalization such as OLS and SRG that are employed to "soften" the realistic interactions, which in turn can be used in comparatively smaller model space. In short, these techniques transform the two-body Hamiltonian into an effective Hamiltonian for given A that decouples from high-energy physics, while preserving the symmetries of the initial Hamiltonian. The OLS technique is described in detail in Ref. [25], whereas specific details for the SRG are available in Ref. [26].

Comparing the SU(3) decompositions of initial interactions to their renormalized (effective) counterparts shows that the same major SU(3) tensors remain dominant after renormalization (Fig. 1). In the case of JISP16 the tensors with the largest relative strengths practically do not change. The renormalization has a larger impact on the N3LO interaction where the spread over various tensors is larger. Here, only a few SU(3)-symmetric components change significantly while the others change slightly. It should be noted that the two effective counterparts of the interactions resemble each other (Fig. 1). A similar behavior is observed for, e.g., the AV18 [44] and CD-Bonn interactions [21].

Examining the largest contributing tensors of realistic interactions, we can link them to the monopole operator (the HO potential), $Q \cdot Q$, spin-orbit, pairing, and tensor forces. The key idea is that the position and momentum operators, $\vec{r}$ and $\vec{p}$ respectively, have an SU(3) rank (1 0), and conjugate (0 1) (to preserve Hermiticity), with $\text{SU}(2)_S$ rank zero ($S_0 = 0$, that is, the operator does not change spin). The HO potential operator ($\sim r^2 = \vec{r} \cdot \vec{r}$) has orbital momentum $L_0 = 0$ and spin $S_0 = 0$, and its SU(3) rank is obtained by coupling (1 0) × (1 0), (1 0) × (0 1) and conjugates. For $L_0 = 0$, the SU(3) Clebsch-Gordan coefficients for these couplings are nonzero only for total $(\lambda_0\, \mu_0) = (2\,0), (0\,2)$ that, in turn, define the SU(3) ranks of the HO potential.

The quadrupole operator Q, given by the tensor product of $\vec{r}$, has $L_0 = 2$ and $S_0 = 0$. Here, the SU(3) Clebsch-Gordan coefficients restrict the total $(\lambda_0\, \mu_0)$ to (2 0) and (1 1) (and conjugates), which define the SU(3) rank of Q [19]. Consequently, the $Q \cdot Q$ operator, which describes the interaction of each nucleon with the quadrupole moment of the nucleus, will have $L_0 = 0$ and spin $S_0 = 0$, along with SU(3) rank of (4 0), (2 0), (2 2), and (0 0) (and conjugates). Similarly, the spin-orbit operator has $(\lambda_0\, \mu_0) = (1\,1)$, $L_0 = 1$ from the orbital momentum operator and $S_0 = 1$ from the spin operator.

The idea of the pairing interaction in nuclei is that the configurations with paired nucleons are energetically favored. The SU(3) ranks of the pairing interaction are derived in

Ref. [45], which shows that a large number of pairing interaction tensors have $\lambda_0 = \mu_0$ SU(3) rank. Last, the nuclear tensor force originates mainly from the one-pion exchange and it depends on the orientation of the spins with regard to the relative coordinate vector joining the two nucleons (see, e.g., Ref. [46]). Similarly to the quadrupole operator, the tensor force has $L_0 = 2$ and SU(3) rank of (2 0) and (1 1) (and conjugates), but with $S_0 = 2$, coming from the tensor coupling of the spin operators.

Indeed, the scalar $(0\,0)S_0 = 0$ dominates for a variety of realistic interactions, and especially in their effective counterparts (see Fig. 1). As mentioned above, this suggests a dominant Elliott SU(3) symmetry. This may have important implications for various models that employ the SU(3) symmetry, such as the ones is Refs. [47–53]. The next important components are typically (2 0), (4 0), and $(2\,2)S_0 = 0$ and their conjugates. These SU(3) modes are the ones that appear in the $Q \cdot Q$ interaction, while $(\lambda_0\,\lambda_0)$ configurations dominate the pairing interactions within a shell [45]. The dominant (2 0) and $(1\,1)S_0 = 2$ modes, and conjugates, can be linked to the tensor force. Finally, the $(1\,1)S_0 = 1$ can be linked to the spin-orbit force. These features, we find, repeat for various realistic interactions and, more notably, the similarity is found to be further enhanced for their renormalized counterparts. Given the link between the phenomenon-tailored interactions and major terms in realistic interactions, it is then not surprising that both *ab initio* approaches and earlier schematic models can successfully describe dominant features in nuclei.

IV. CONCLUSIONS

Realistic NN interactions expressed in SU(3) basis show a clear dominance of only a small fraction of terms. We performed *ab initio* calculations of several observables in ^{12}C using interactions that were selected down to the most significant terms and compared them to the calculations with the initial interactions. We found that for the small $\hbar\Omega$ values even the interactions with less than half of the terms produce almost the same results as the initial interaction for the low-lying spectrum, $B(E2)$ values, and rms radii of ^{12}C. The selection appears to affect more the calculations that use interactions with higher $\hbar\Omega$ values in small model spaces; however, the deviations between the initial and selected interaction results decrease as the model space becomes larger. In addition, the eigenvalues of the proton-neutron system for all of the positive and negative parity states below 30 MeV change only slightly with as few as the quarter of the initial interaction terms.

By analyzing the most dominant terms of various realistic interactions, we found that they can be linked to well known nuclear forces. In particular, inspection of these terms allowed us to link them to the widely used HO potential, $Q \cdot Q$, pairing, spin-orbit, and tensor forces. Moreover, we saw that after renormalization the NN interactions, regardless of their type, have mainly the same dominant terms with similar strengths, indicating that the renormalization techniques strengthen the same dominant terms in all interactions.

ACKNOWLEDGMENTS

Support from the US National Science Foundation (Grants No. ACI-1713690, No. OIA-1738287, No. PHY-1913728), the US Department of Energy (Grant No. DE-FG02-93ER40756), the Czech Science Foundation (Grant No. 16-16772S), and the Southeastern Universities Research Association are all gratefully acknowledged. This work benefited from computing resources provided by NSF's Blue Waters computing system (NCSA), LSU [54], and the National Energy Research Scientific Computing Center (NERSC).

APPENDIX

In standard second quantized form, a one- and two-body interaction Hamiltonian is given in terms of fermion creation $a^\dagger_{jm(1/2)\sigma}$ and annihilation $\tilde{a}_{j-m(1/2)-\sigma} = (-1)^{j-m+1/2-\sigma} a_{jm(1/2)\sigma}$ tensors, which create or annihilate a particle of type $\sigma = \pm 1/2$ (proton or neutron) in the HO basis.

In Eq. (A1), V^Γ_{rstu} is the two-body antisymmetric matrix element in the JT-coupled scheme $[V^\Gamma_{rstu} = -(-)^{r+s-\Gamma} V^\Gamma_{srtu} = -(-)^{t+u-\Gamma} V^\Gamma_{rsut} = (-)^{r+s-t-u} V^\Gamma_{srut} = V^\Gamma_{turs}]$. For an isospin nonconserving two-body interaction of isospin rank $\mathcal{T}$, the coupling of fermion operators is $\{\{a^\dagger_r \times a^\dagger_s\}^{JT} \times \{a_t \times a_u\}^{JT}\}^{(0\mathcal{T})}$, with $V^{(\mathcal{T})JT}_{rstu}$ matrix elements

$$
\begin{aligned}
V &= -\frac{1}{4} \sum_{rstu\Gamma} \sqrt{(1+\delta_{rs})(1+\delta_{tu})}\, \Pi_\Gamma V^\Gamma_{rstu} \{\{a^\dagger_r \times a^\dagger_s\}^\Gamma \times \{\tilde{a}_t \times \tilde{a}_u\}^\Gamma\}^{(\Gamma_0 M_{\Gamma_0})} \\
&= \sum_{\substack{(\chi^* \omega S)_{fi} \\ \rho_0 \omega_0 \kappa_0 S_0}} \frac{(-1)^{\omega_0 - \omega_f + \omega_i}}{\sqrt{(1+\delta_{\eta_r \eta_s})(1+\delta_{\eta_t \eta_u})}} \frac{1}{\Pi_{S_0}} \sqrt{\frac{\dim \omega_f}{\dim \omega_0}} V^{\rho_0 \omega_0 \kappa_0 S_0}_{(\chi \omega S)_{f,i} T} \\
&\quad \times \sum_{\rho_0'} \Phi_{\rho_0' \rho_0}(\omega_0 \omega_i \omega_f) \{\{a^\dagger_{\eta_r} \times a^\dagger_{\eta_s}\}^{\omega_f S_f T} \times \{\tilde{a}_{\eta_t} \times \tilde{a}_{\eta_u}\}^{\omega_i S_i T}\}^{\rho_0' \omega_0 \kappa_0 (L_0 = S_0 S_0) \Gamma_0 = 0 M_{\Gamma_0} = 0},
\end{aligned}
\tag{A1}
$$

where $\dim \omega$ is defined in Eq. (3) and the phase matrix $\Phi_{\rho_0' \rho_0}(\omega_0 \omega_i \omega_i)$ accommodates the interchange between the coupling of ω_0 and ω_i to ω_f, so for SU(3) Clebsch-Gordan coefficients we have [55]

$$
\langle \omega_0 \kappa_0 L_0 M_0; \omega_i \kappa_i L_i M_i |\, \omega_f \kappa_f L_f M_f \rangle_{\rho_0} = \sum_{\rho_0'} \Phi_{\rho_0 \rho_0'}(\omega_0 \omega_i \omega_f) \langle \omega_i \kappa_i L_i M_i; \omega_0 \kappa_0 L_0 M_0 |\, \omega_f \kappa_f L_f M_f \rangle_{\rho_0'}. \tag{A2}
$$

For the special case when $\rho = 1$, that is, where the SU(3) coupling $\{\omega_i \times \omega_0\} \to \omega_f$ is unique, the phase matrix reduces to a simple phase factor $(-1)^{(\lambda_0+\mu_0)+(\lambda_i+\mu_i)-(\lambda_f+\mu_f)}$. Finally, the interaction reduced matrix elements in a SU(3) × SU(2)$_S$ × SU(2)$_T$-coupled HO basis are given as

$$
\begin{aligned}
V^{\rho_0\omega_0\kappa_0 S_0}_{(\chi\omega S)_{fi};T} &= (-)^{S_f+S_0}\Pi_{TS_0}\frac{\dim\omega_0}{\dim\omega_f}\sum_{J(\kappa L)_{if}}(-)^{L_i+J}\Pi_J^2\Pi_{L_f}\begin{Bmatrix} L_f & S_f & J\\ S_i & L_i & S_0\end{Bmatrix}\langle\omega_i\kappa_i L_i;\omega_0\kappa_0 L_0\|\omega_f\kappa_f L_f\rangle_{\rho_0}V^{\Gamma}_{(\chi\omega\kappa LS)_{fi}}\\
&= (-)^{S_f+S_0}\Pi_{TS_0}\frac{\dim\omega_0}{\dim\omega_f}\sum_{J(\kappa L)_{if}}(-)^{L_i+J}\Pi_J^2\Pi_{L_f}\begin{Bmatrix} L_f & S_f & J\\ S_i & L_i & S_0\end{Bmatrix}\langle\omega_i\kappa_i L_i;\omega_0\kappa_0 L_0\|\omega_f\kappa_f L_f\rangle_{\rho_0}\\
&\times\Pi_{L_iL_fS_iS_f}\sum_{\substack{l_rl_sl_tl_u\\ j_rj_sj_tj_u}}\sqrt{\frac{(1+\delta_{rs})(1+\delta_{tu})}{(1+\delta_{\eta_r\eta_s})(1+\delta_{\eta_t\eta_u})}}\Pi_{j_rj_sj_tj_u}\langle(\eta_r\,0)l_r;(\eta_s\,0)l_s\|(\omega\kappa L)_f\rangle\\
&\times\langle(\eta_t\,0)l_t;(\eta_u\,0)l_u\|(\omega\kappa L)_i\rangle\begin{Bmatrix} l_r & \frac{1}{2} & j_r\\ l_s & \frac{1}{2} & j_s\\ L_f & S_f & J\end{Bmatrix}\begin{Bmatrix} l_t & \frac{1}{2} & j_t\\ l_u & \frac{1}{2} & j_u\\ L_i & S_i & J\end{Bmatrix}V^{\Gamma}_{rstu},
\end{aligned}
\tag{A3}
$$

where $V^{\Gamma}_{(\chi\omega\kappa LS)_{fi}}$ is a two-body interaction in a SU(3)-JT-coupled scheme; as mentioned above $\langle;\|\rangle$ are reduced SU(3) Clebsch-Gordan coefficients [33,34], and we use SU(2) Wigner 6-j and 9-j symbols.

[1] R. Machleidt, K. Holinde, and C. Elster, Phys. Rep. **149**, 1 (1987).
[2] R. Machleidt, in *Advances in Nuclear Physics*, edited by J. W. Negele and E. Vogt (Springer, Berlin, 1989), Vol. 19, pp. 189–376.
[3] R. Machleidt, Phys. Rev. C **63**, 024001 (2001).
[4] U. van Kolck, Phys. Rev. C **49**, 2932 (1994).
[5] E. Epelbaum, H.-W. Hammer, and U.-G. Meißner, Rev. Mod. Phys. **81**, 1773 (2009).
[6] R. Machleidt and D. R. Entem, Phys. Rep. **503**, 1 (2011).
[7] A. Ekström, G. Baardsen, C. Forssén, G. Hagen, M. Hjorth-Jensen, G. R. Jansen, R. Machleidt, W. Nazarewicz, T. Papenbrock, J. Sarich *et al.*, Phys. Rev. Lett. **110**, 192502 (2013).
[8] D. R. Entem and R. Machleidt, Phys. Rev. C **68**, 041001(R) (2003).
[9] A. Shirokov, J. Vary, A. Mazur, and T. Weber, Phys. Lett. B **644**, 33 (2007).
[10] A. Shirokov, V. Kulikov, P. Maris, A. Mazur, E. Mazur, and J. Vary, EPJ Web Conf. **3**, 05015 (2010).
[11] J. P. Elliott, Proc. R. Soc. A **245**, 128 (1958).
[12] J. P. Elliott, Proc. R. Soc. A **245**, 562 (1958).
[13] J. P. Elliott and M. Harvey, Proc. R. Soc. A **272**, 557 (1962).
[14] A. Bohr and B. R. Mottelson, *Nuclear Structure* (Benjamin, New York, 1969), Vol. 1.
[15] G. Racah, Phys. Rev. **62**, 438 (1942).
[16] S. T. Belyaev, Fys. Medd. **31** (1959).
[17] R. Richardson and N. Sherman, Nucl. Phys. **52**, 253 (1964).
[18] A. C. Dreyfuss, K. D. Launey, T. Dytrych, J. P. Draayer, and C. Bahri, Phys. Lett. B **727**, 511 (2013).
[19] G. K. Tobin, M. C. Ferriss, K. D. Launey, T. Dytrych, J. P. Draayer, A. C. Dreyfuss, and C. Bahri, Phys. Rev. C **89**, 034312 (2014).
[20] M. E. Miora, K. D. Launey, D. Kekejian, F. Pan, and J. P. Draayer, Phys. Rev. C **100**, 064310 (2019).
[21] K. D. Launey, T. Dytrych, and J. P. Draayer, Prog. Part. Nucl. Phys. **89**, 101 (2016).
[22] T. Dytrych, K. D. Launey, J. P. Draayer, D. J. Rowe, J. L. Wood, G. Rosensteel, C. Bahri, D. Langr, and R. B. Baker, Phys. Rev. Lett. **124**, 042501 (2020).
[23] A. C. Dreyfuss, K. D. Launey, T. Dytrych, J. P. Draayer, R. B. Baker, C. M. Deibel, and C. Bahri, Phys. Rev. C **95**, 044312 (2017).
[24] S. Okubo, Prog. Theor. Phys. **12**, 603 (1954).
[25] K. Suzuki and S. Y. Lee, Prog. Theor. Phys. **64**, 2091 (1980).
[26] S. K. Bogner, R. J. Furnstahl, and R. J. Perry, Phys. Rev. C **75**, 061001(R) (2007).
[27] C. W. Johnson, Phys. Rev. Lett. **124**, 172502 (2020).
[28] P. Navrátil, J. P. Vary, and B. R. Barrett, Phys. Rev. Lett. **84**, 5728 (2000).
[29] P. Navrátil, J. P. Vary, and B. R. Barrett, Phys. Rev. C **62**, 054311 (2000).
[30] D. H. Gloeckner and R. D. Lawson, Phys. Lett. B **53**, 313 (1974).
[31] T. Dytrych, P. Maris, K. D. Launey, J. P. Draayer, J. P. Vary, M. Caprio, D. Langr, U. Catalyurek, and M. Sosonkina, Comput. Phys. Commun. **207**, 202 (2016).
[32] J. P. Draayer, Y. Leschber, S. C. Park, and R. Lopez, Comput. Phys. Commun. **56**, 279 (1989).
[33] Y. Akiyama and J. P. Draayer, Comput. Phys. Commun. **5**, 405 (1973).
[34] J. P. Draayer and Y. Akiyama, J. Math. Phys. **14**, 1904 (1973).
[35] F. Ajzenberg-Selove and J. Kelley, Nucl. Phys. A **506**, 1 (1990).
[36] K. Hecht and J. Draayer, Nucl. Phys. A **223**, 285 (1974).
[37] J. B. French, Phys. Lett. **23**, 248 (1966).
[38] J. B. French and K. F. Ratcliff, Phys. Rev. C **3**, 94 (1971).
[39] F. S. Chang, J. B. French, and T. H. Thio, Ann. Phys. (NY) **66**, 137 (1971).
[40] V. K. B. Kota and R. U. Haq, *Spectral Distributions in Nuclei and Statistical Spectroscopy* (World Scientific, Singapore, 2010).
[41] K. D. Launey, S. Sarbadhicary, T. Dytrych, and J. P. Draayer, Comput. Phys. Commun. **185**, 254 (2014).

[42] I. Tanihata, H. Hamagaki, O. Hashimoto, Y. Shida, N. Yoshikawa, K. Sugimoto, O. Yamakawa, T. Kobayashi, and N. Takahashi, Phys. Rev. Lett. **55**, 2676 (1985).
[43] D. J. Rowe, Phys. Rev. C **101**, 054301 (2020).
[44] R. B. Wiringa, V. G. J. Stoks, and R. Schiavilla, Phys. Rev. C **51**, 38 (1995).
[45] C. Bahri, J. Escher, and J. Draayer, Nucl. Phys. A **592**, 171 (1995).
[46] T. Otsuka, T. Suzuki, R. Fujimoto, H. Grawe, and Y. Akaishi, Phys. Rev. Lett. **95**, 232502 (2005).
[47] M. Harvey, in *Advances in Nuclear Physics*, edited by M. Baranger and E. Vogt (Springer, Boston, MA, 1968), Vol. 1, pp. 67–182.
[48] R. R. Raju, J. Draayer, and K. Hecht, Nucl. Phys. A **202**, 433 (1973).
[49] A. P. Zuker, J. Retamosa, A. Poves, and E. Caurier, Phys. Rev. C **52**, R1741(R) (1995).
[50] C. Vargas, J. Hirsch, and J. Draayer, Nucl. Phys. A **690**, 409 (2001).
[51] G. Popa, J. G. Hirsch, and J. P. Draayer, Phys. Rev. C **62**, 064313 (2000).
[52] T. Beuschel, J. P. Draayer, D. Rompf, and J. G. Hirsch, Phys. Rev. C **57**, 1233 (1998).
[53] A. Martinou, D. Bonatsos, N. Minkov, I. Assimakis, S. Peroulis, S. Sarantopoulou, and J. Cseh, Eur. Phys. J. A **56**, 239 (2020).
[54] http://www.hpc.lsu.edu.
[55] J. Escher, Ph.D. thesis, Louisiana State University, 1997.